1-G MODEL TEST ON PILE-SOIL INTERACTION IN LATERAL FLOW OF LIQUEFIED GROUND

J. Kuwano[1)], A. Takahashi[2)], Y. Yano[3)] and T. Saruwatari[4)]

1) Associate Professor, Department of Civil Engineering, Tokyo Institute of Technology, Japan
2) Research Associate, Dept. of Civil and Environmental Engineering, Imperial College, London, U.K.
3) Mitsubishi Jisho Sekkei Inc., Tokyo, Japan
4) Graduate Student, Department of Civil Engineering, Tokyo Institute of Technology, Japan
jkuwano@cv.titech.ac.jp

Abstract: This paper describes an experimental study on lateral resistance of a pile in liquefied sand. In order to avoid complication in interpretation of the test results and to easily observe the behavior of soil surrounding the pile, the pile was modeled as a buried cylinder that corresponded to a sectional model of the pile at a certain depth in subsoil. The deformation of the soil surrounding the cylinder was successfully observed by digital video camera. Loading rate effects on the lateral resistance of the cylinder was also investigated.

1. INTRODUCTION

Detailed observations on damage of pile foundations after the Hyogo-ken Nambu Earthquake of 1995 revealed that pile cracking and structure hinging occurred at the pile cap or the interfaces between soil layers having different lateral stiffness (e.g. Matsui & Oda, 1996; Fujii et al., 1998). This kind of damage was mainly found in sites where liquefaction took place particularly when large lateral movements of liquefied soil overlaid non-liquefied soil occurred.

The effects of large lateral soil movement, especially liquefaction-induced lateral spreading of soil, on the failure and deformation of the piles have been experimentally investigated using geotechnical centrifuges by many researchers (e.g. Abdoun & Dobry, 1998; Horikoshi et al., 1998; Satoh et al., 1998; Takahashi et al., 1998). In these researches, shaking tables were used to simulate the ground motions during earthquakes. Information derived from the shaking table tests is seen to be of value in demonstrating the actual behavior of piles and soils during earthquakes. However, the actual behavior of piles is complicated and affected by several factors. Investigating the effect of each factor from the complicated behavior observed in the shaking table tests is not a straightforward process.

In order to avoid this complication in their interpretation and to easily observe the soil surrounding the pile, the pile was modeled as a buried cylinder that corresponded to a sectional model of the pile at a certain depth in subsoil (Fig.1). Based on almost the same concept, measurement of the drag force of the buried cylinder embedded in sand was carried out by Towhata et al. (1999). However, as their tests were conducted under very low initial over burden pressure, it is very difficult to make a comparison between the test results and actual phenomena observed in the field. In order to create a realistic stress condition in the model ground, the model was prepared in a sealed container and the over burden pressure was applied to the ground surface by a rubber pressure bag.

This paper focuses on observing the deformation of the liquefied soil surrounding the pile when a large relative displacement between the pile and the soil is induced. The loading rate effect on the lateral resistance of the pile in the liquefied sand is also investigated.

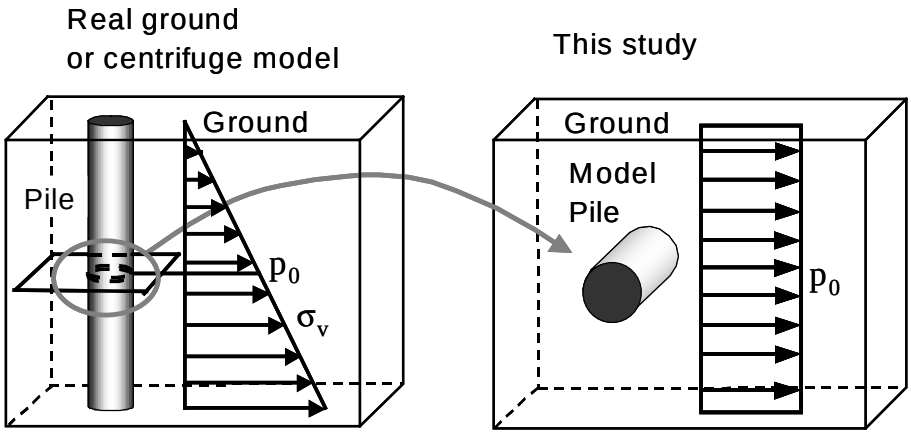

Figure 1. Modeling of pile in this study.

2. TEST PROCEDURES AND CONDITIONS

2.1 Test procedures

The model setup used in this study is schematically illustrated in Fig.2. An aluminum model container was used with inner sizes of 450mm in width, 150mm in breadth, and 250mm in height. The front face of the box was a transparent window to allow observing deformation of the model ground. A pressure bag made of rubber was attached underneath the top lid of the container to apply an over burden pressure, P_A, on the surface of the soil. A fluid tank was connected to the bottom of the box to supply and drain out fluid and to apply back pressure, P_B, to the pore fluid of the soil.

Figure 3 shows an aluminum-made-cylinder equipped with pore and earth pressure transducers. The surface of the cylinder was made smooth by the fabricator. Rubber sheets were put on both ends of the cylinder for lubrication and to prevent sand particles from getting into the gap between the cylinder and the side walls of the container. Two rods were connected to the center of the cylinder. Two load cells were inserted into the respective rods near the cylinder to avoid the influence of friction in measuring the net lateral force on the cylinder. The cylinder was actuated back and forth through the rods by an electro-hydraulic actuator. The actuator was mounted on the side wall of the model container.

Toyoura sand, uniformly graded sub-angular quartz sand (D_{50}=0.19mm) was used for the

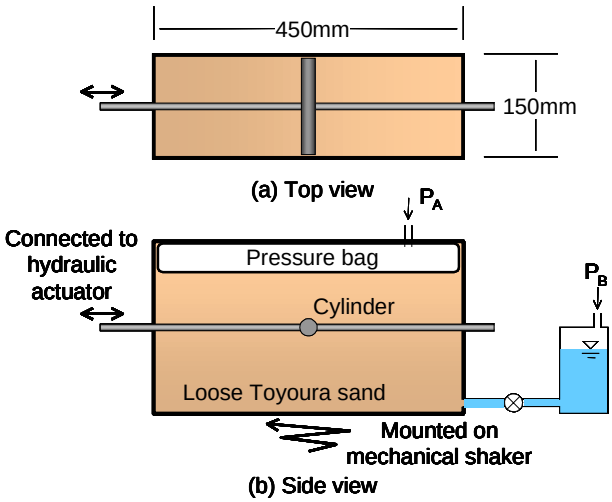

Figure 2. Schematic illustration of model

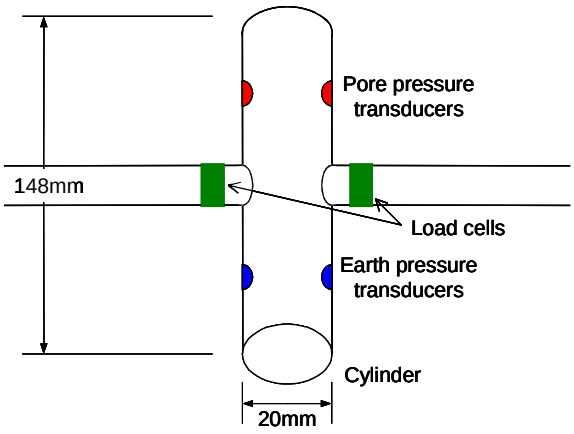

Figure 3. Schematic illustration of cylinder

Table 1. Test conditions.

Case	Pore fluid material	Back pressure P_B (kPA)	Cylinder loading rate V (mm/s)	Shaking
SW1Q	water	49	1 (monotonic)	X
SW10Q	water	49	10 (monotonic)	X
SW1	water	0	1 (monotonic)	O
SW10	water	0	10 (monotonic)	O
SW100	water	0	100 (cyclic)	O
SM1	methyl cel. sol.	0	1 (cyclic)	O
SM10	methyl cel. sol.	0	10 (cyclic)	O
SM100	methyl cel. sol.	0	100 (cyclic)	O
SM10N	methyl cel. sol.	0	10 (cyclic)	X
SM100N	methyl cel. sol.	0	100 (cyclic)	X

model. The model was prepared by the air pluviation method to achieve the relative density of 30~40%. It was saturated up to the ground surface with de-aired water or methyl cellulose solution under a negative pressure of 98kPa in a large tank by applying a vacuum. Japanese noodles `somen' were placed between the model ground and the transparent window as markers to observe deformation of the ground. After the saturation, the top lid of the box was attached and the over burden pressure was applied to the soil under the drained condition.

Having prepared the model, the model container was set on the mechanical shaker and the electro-hydraulic actuator was attached to the container. In the tests, the horizontal shaking of the container started two seconds prior to the pile loading. This duration was enough to liquefy the model ground. A horizontal shaking was applied to the container by sinusoidal waves with a frequency of 50Hz and a maximum acceleration of approximately 5g. A period of shaking was 10 seconds. During the tests, acceleration of the container, horizontal load and displacement of the cylinder and earth pressure and pore fluid pressure around the cylinder were measured. Movement of the cylinder and the ground was recorded by a digital video camera.

2.2 Test Conditions

Table 1 shows the test conditions in this study. Effects of the ground vibration and the loading rate of the cylinder on the lateral resistance of the cylinder were investigated. In all the cases, the applied over burden pressure was P_A=49kPa. The loading rate of the cylinder, V, was varied from 1mm/s to 100mm/s. In the cyclic loading tests, the symmetrical triangular waves were applied in order to achieve a constant loading rate.

In cases SW1, SW10, SW100, SM1, SM10 and SM100, a horizontal sinusoidal motion was applied to the container to generate the excess pore fluid pressure in the model. Meanwhile, in cases SW1Q and SW10Q, pore pressure increase P_B of 49kPa was applied to the soil after the consolidation of the soil at P_A=49kPa without ground vibration. The effective confining stress of the model became almost zero by increasing the back pressure without ground vibration on the condition that the model was subjected to almost the same stress history that the models in the other cases experienced. This stress condition is defined as artificial soil “liquefaction without ground vibration” in this study. SM1N and SM100N were the tests in which the cylinder was moved back and forth with the initial condition of no liquefaction.

At the beginning, de-aired water was used as the pore fluid. However, considering the partial drainage around the cylinder, the migration velocity of water was relatively large, as the diameter of

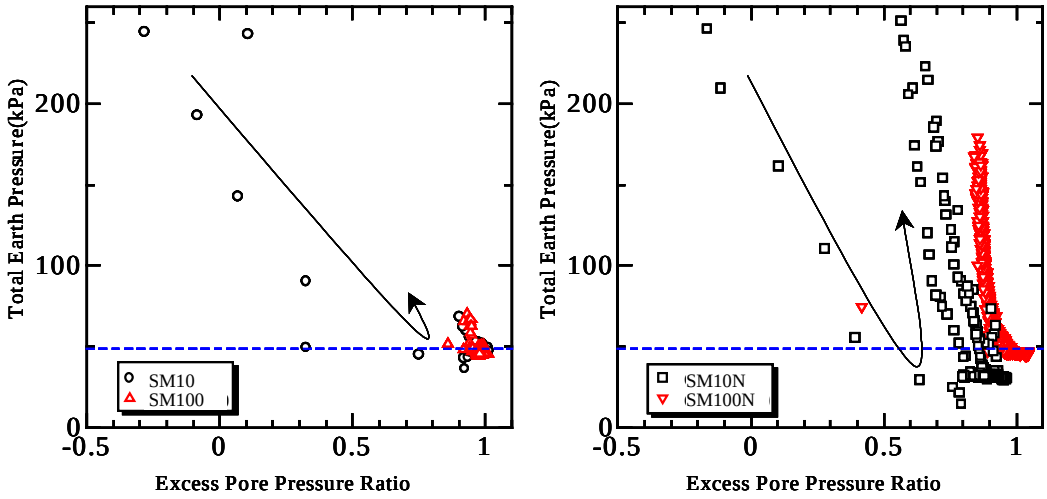

Figure 4. Total earth pressure vs. excess pore pressure on the cylinder surface (SM10, SM100, SM10N & SM100N).

the cylinder was very small compared with the actual pile. In order to resolve the problem, in the latter half of the series of the tests, the scaling laws of the centrifuge modeling were adopted, i.e. a higher viscosity fluid (methyl cellulose solution) was used as the pore fluid to avoid conflict with the scaling laws for the time of dynamic events and seepage. The viscosity of the methyl cellulose solution was 50 times higher than that of fresh water. With this similitude rule, measured lateral resistance of the 20mm-diameter cylinder corresponds to the lateral resistance of the 1m-diameter pile at a depth of 5m. Loading rate of 1mm/s corresponds to the situation of the pile in a very slow flow of liquefied soil, while that of 100mm/s corresponds to the vibration of the pile during an earthquake.

3. TEST RESULTS AND DISCUSSIONS

3.1 Earth Pressure and Lateral Resistance on the Cylinder with Excess Pore Pressure

Total earth pressure is plotted against excess pore pressure ratio in Fig.4 for the cases of SM10, SM100, SM10N and SM100N. Pressures shown here are measured on the initially loaded side surface of the cylinder and the excess pore pressure is normalized by the initial over burden pressure, $p_0=P_A$. In case SM10, total earth pressure drastically increased in the first cycle, associated with negative excess pressure. Total earth pressure then converged almost 49 kPa in the following cycles in which excess pore pressure ratio was kept almost 1. In case SM10N also, the total earth pressure increased rapidly with the excess pore pressure drop caused by dilative behavior of soil with the movement of pile. Unlike SM10, the total earth pressure increased and decreased repeatedly in the following cycles. However, when the excess pore pressure ratio increased to be over 0.9, the total earth pressure kept almost constant value of 49 kPa without showing dilative behavior of solid ground. The ground behaved like liquid. Cases SM100 and SM100N showed almost the same tendency.

Lateral resistances of cylinder against displacement in cases SW1Q, SW10Q, SW1 and SW10 are plotted in Fig.5. The lateral resistance is the lateral force acting on the cylinder divided by a projected area of the cylinder on a vertical plane. Lateral forth is the difference of forces measured by the load cells on the left and right rods. In the figure, lateral resistance, p, and displacement of the cylinder, δ, are normalized by an initial over burden pressure, $p_0=P_A$, and the diameter of the cylinder, D, respectively. Herein the normalized displacement, δ/D, is called the reference strain, γ. Irrespective of the method inducing liquefaction, the larger loading rate makes the lateral resistance larger. Further discussion on the loading rate effect will be made later.

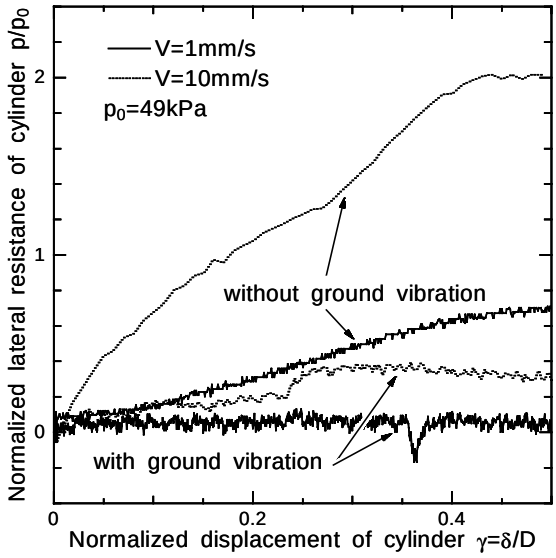

Figure 5. Lateral resistance against lateral displacement of cylinder (SW1Q, SW10Q, SW1 & SW10).

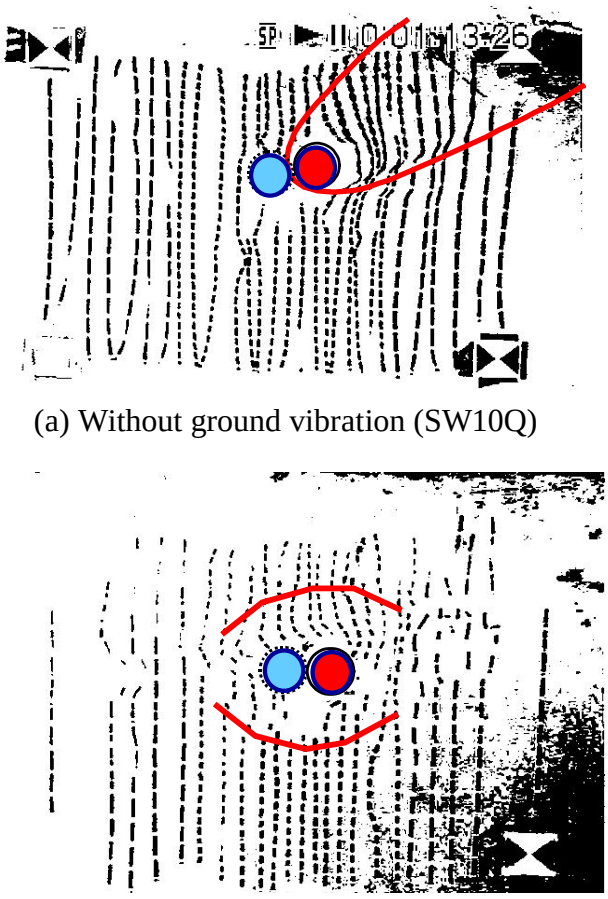

(a) Without ground vibration (SW10Q)

(b) With ground vibration (SW10)

Figure 6. Deformation of surrounding soil just after loading.

Regarding the difference in the method used to induce liquefaction, the lateral resistances for the cases without vibration of the ground are remarkably larger than those for the cases with vibration. Fig.6 shows observed deformation of the soil surrounding the cylinder just after loading. The black lines are noodle markers placed vertically on the soil before the tests. Without ground vibration, the large amount of soil in front of the cylinder moved forward resulting in a heaving of the ground surface of the front side. On the other hand, when the shaking was applied to the container, deformation of the soil was quite limited in the area adjacent to the cylinder. The difference in the soil area influenced may directly affect the lateral resistance of the cylinder as shown in Fig.5. The vibration of the ground may cause instability in the contacts of the soil particles and reduce the resistance of the surrounding soil against the movement of the cylinder.

3.2 Loading Rate Effects on Lateral Resistance

Figure 7 shows the first loops of the relationship between the lateral resistance and displacement of the cylinder in cases SM1, SM1 0 and SM100. In these cases, the loading rate was varied from 1mm/s to 100mm/s, and the cylinder first moved toward the actuator-side, i.e. the leftward displacement is taken as negative. The initial resistance was negligibly small in all the cases. The larger lateral resistance is mobilized as the loading rate becomes higher. The lateral resistance was mobilized only after a certain amount of displacement was developed depending on the loading rate.

The point where the gradient of the loop starts to increase is here defined as a resistance transformation point. The normalized displacement at the point is referred to as the reference strain of resistance transformation point, γ_L, as shown in Fig.8. This reference strain was originally introduced by Yasuda et al. (1998) as the point that the shear strength of soil starts to recover in a post liquefaction stress-strain relation. Reference strains of resistance transformation point in the first loading are plotted against loading rate in Fig.9. In the case of the smallest loading rate, as no obvious mobilization of the lateral resistance was observed in the range of the pile displacement imposed in

this study, the reference strain must be larger than the value shown in the figure. The smaller loading rate makes the reference strain of resistance transformation point larger. This tendency may be associated with not only the dilatancy characteristics of sand but also pore fluid migration around the cylinder.

Figure 10 shows the time histories of the lateral resistance, the displacement of the cylinder and excess pore fluid pressure around the cylinder in cases SM1 and SM10. It should be noted that the base motion continued only until the end of the first half of the loading cycle in the 1mm/s loading rate case, as the period of the container shaking was 10 seconds. Excess pore fluid pressure of the soil surrounding the cylinder was measured by the pressure transducers attached to the cylinder shown in Fig.3. If we look at the first quarter cycle of the last half of the first loading cycle, in both the cases, the pore pressure on the side of the movement direction (the dotted line) once slightly increased by the sand contraction, then it showed rapid decrease due to the sand dilation. Suction force on the back side of the cylinder, while the pressure on the back side (the solid line) monotonically decreased due to the suction force.

As a result, the pore pressure decreased on both sides when the maximum displacement of the cylinder was imposed, though the pressure on the side of the direction of movement was larger than that on the other side in both the cases.

Comparing the pore pressure responses in SM1 (V=1mm/s) to those in SM10 (V=10mm/s), the decrease in the pore pressure was smaller, and the displacement of the cylinder when the excess pore fluid pressure started to decrease was larger for the smaller loading rate. It is because the suction force on the back side of the cylinder will be small when the hydraulic conductivity of the sand is sufficiently larger than the cylinder loading rate. This difference in pore pressure responses would directly affect the cylinder displacement required for the lateral resistance mobilization, i.e., the reference strain of resistance transformation point shown in Fig.9.

Lateral resistances of the cylinder at $\gamma=\delta/D=0.1$, 0.2, and 0.4 are plotted against cylinder loading rate normalized by the soil

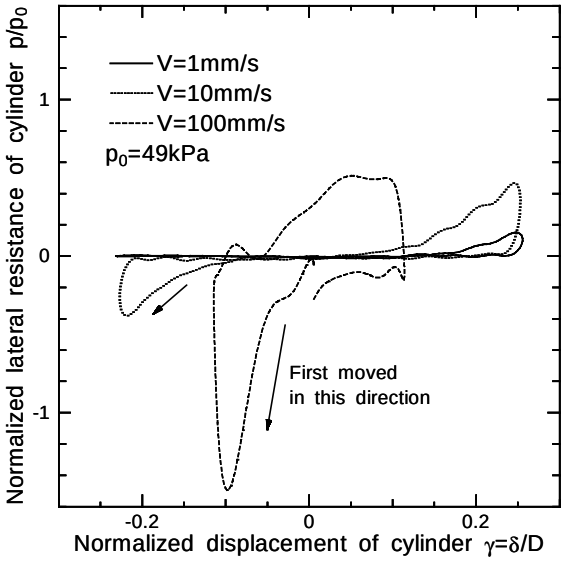

Figure 7. Lateral resistance against lateral displacement of cylinder (SM1-SM100)

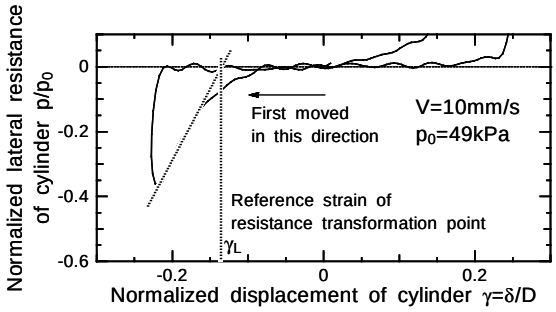

Figure 8. Definition of reference strain of resistance transformation point γ_L

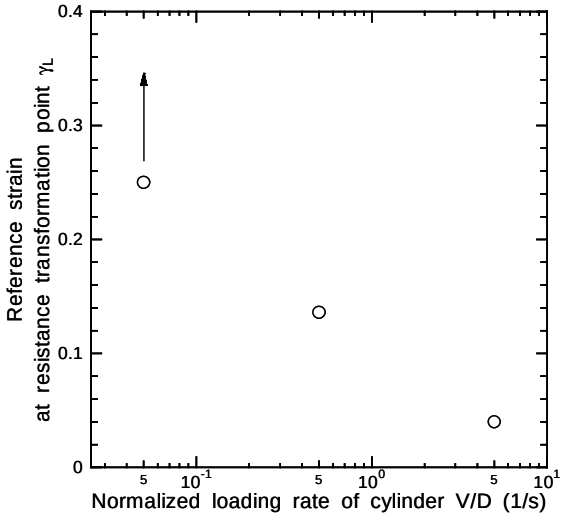

Figure 9. Reference strain of resistance transformation point against loading rate (SM1-SM100)

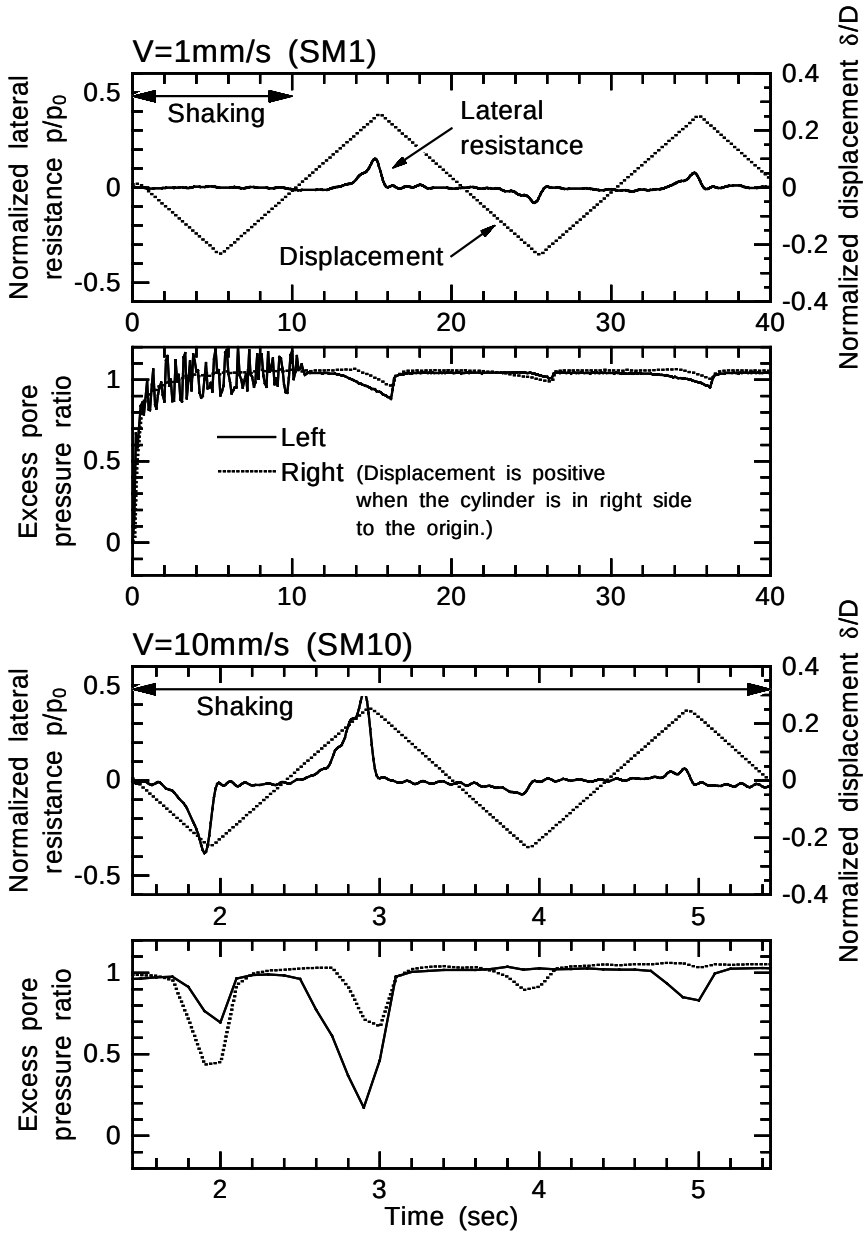

Figure 10. Time histories of lateral resistance and displacement of cylinder and excess pore pressure around cylinder (SM1 & SM10)

hydraulic conductivity in the first loading in Fig.11. The lateral resistance at δ/D=0.1 becomes remarkably larger when $V/k=10^4$. The threshold V/k value for the lateral resistance at δ/D=0.1 exists between 10^3 and 10^4 for the 1m-diameter pile in the medium loose Toyoura sand. This threshold V/k for the lateral resistance varies with δ/D, as the cylinder displacement required for the lateral resistance mobilization depends on V/k. Let us assume piles in a lateral spreading soil that moves 1m in 10 seconds earthquake period, i.e. V=0.1m/s. If the hydraulic conductivity of the liquefied soil is 10^{-5}m/s, V/k becomes 10^4, and the large earth pressure acts on the piles. If k is larger than 10^{-4}m/s, the pressure would become smaller.

All indications in this section support that the pore fluid migration rate, i.e. the hydraulic conductivity of the soil with respect to the loading rate, is the crucial factor for mobilization of the lateral resistance of a buried structure in liquefied soil.

4. CONCLUSIONS

Lateral loading tests on the buried cylinder were conducted to study the lateral resistance of a pile in liquefied soil, focusing on observation of the deformation of the liquefied soil surrounding the pile when a large relative displacement between the pile and the soil is induced. The loading rate effect on the lateral resistance of pile in the liquefied soil was also investigated. The following conclusions were obtained in this study:

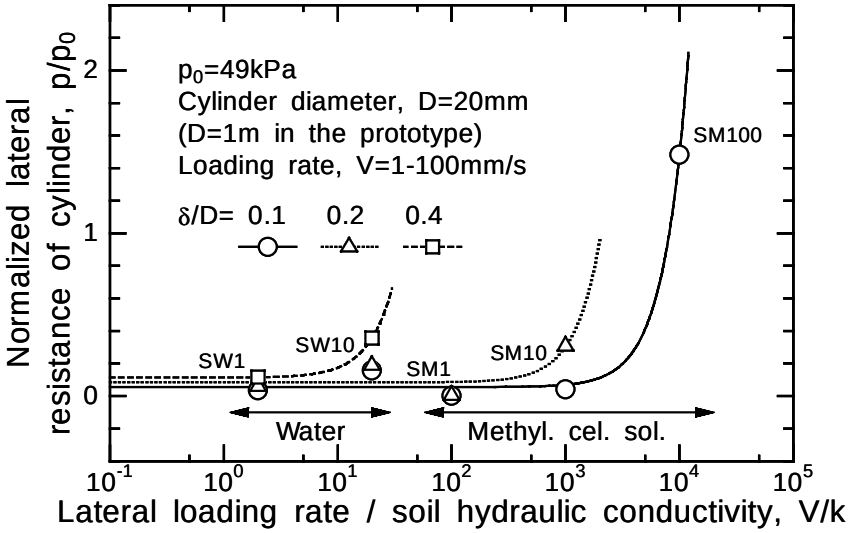

Figure 11. Relationship between lateral resistance of cylinder at δ/D=0.1, 0.2 & 0.4 and cylinder loading rate over soil hydraulic conductivity in first loading.

1) The deformation of the soil surrounding the cylinder could be successfully observed by the digital video camera through the transparent windows of the box.

2) Without ground vibration, the large amount of the soil in front of the cylinder moved forward, while the deformation of the soil was quite limited in the vicinity of the cylinder when shaking was applied to the model container.

3) The difference in the deformation mode of the soil affected the lateral resistance of the cylinder.

4) Larger lateral resistance is mobilized as the loading rate becomes higher.

5) When the loading rate is higher, the cylinder displacement required for the lateral resistance mobilization becomes smaller.

6) Tendencies of loading rate effect are associated with not only the dilatancy characteristics of sand but also pore fluid migration around the cylinder.

7) All indications in this study support that the hydraulic conductivity of the soil in relation to the loading rate is the important factor for the mobilization of the lateral resistance of piles in liquefied soils.

References:

Abdoun, A. and Dobry, R. (1998), "Seismically induced lateral spreading of two-layer sand deposit and its effect on pile foundations," *Proceedings of the International Conference Centrifuge 98*, **1**, 321-328.

Fujii, S., Isemoto, N., Satou, Y., Kaneko, O., Funahara, H., Arai, T. and Tokimatsu, K. (1998), "Investigation and analysis of a pile foundation damaged by liquefaction during the 1995 Hyogoken-Nambu Earthquake," *Soils and Foundations*, Special Issue on Geotechnical Aspects of the Jan. 17 1995 Hyogoken-Nambu Earthquake, (2), 179-192.

Horikoshi, K., Tateishi, A. and Fujiwara, T. (1998), "Centrifuge modeling of a single pile subjected to liquefaction-induced lateral spreading," *Soils and Foundations*, Special Issue on Geotechnical Aspects of the Jan. 17 1995 Hyogoken-Nambu Earthquake, (2), 193-208.

Matsui, T. and Oda, K. (1996), "Foundation damage of structures," *Soils and Foundations*, Special Issue on Geotechnical Aspects of the Jan. 17 1995 Hyogoken-Nambu Earthquake, (1), 189-200.

Satoh, H., Ohbo, N. and Yoshizako, K. (1998), "Dynamic test on behavior of pile during lateral ground," *Proceedings of the International Conference Centrifuge 98*, **1**, 327-332.

Takahashi, A., Takemura, J., Kawaguchi, Y., Kusakabe, O. and Kawabata, N. (1998), "Stability of piled pier subjected to lateral flow of soils during earthquake," *Proceedings of the International Conference Centrifuge 98*, **1**, 365-370.

Towhata, I., Vargas-Mongem W., Orense, R.P. and Yao, M. (1999), "Shaking table tests on subgrade reaction of pipe embedded in sandy liquefied subsoil," *Soil Dynamics and Earthquake Engineering*, **18**(5), 347-361.

Yasuda, S., Terauchi, T., Morimoto, H., Erken, A. and Yoshida, N. (1998), "Post liquefaction behavior of several sands," *Proceedings of the 11th European Conference on Earthquake Engineering*.